Transition Metal Chemistry
https://doi.org/10.1007/s11243-018-00293-0

The formation of dinuclear trichloro-bridged and mononuclear ruthenium complexes from the reactions of dichlorotris(*p*-tolylphosphine)ruthenium(II) with diazabutadiene ligands

Meng Guan Tay[1] · Ying Ying Chia[1] · Suzie Hui Chin Kuan[1] · Tze Pei Phan[1]

Received: 18 September 2018 / Accepted: 24 November 2018

Abstract
Ru(II) complexes with diazabutadiene (R-DAB) ligands have been prepared. The reaction of $RuCl_3{\cdot}nH_2O$ with P(*p*-tolyl)$_3$ gave a [$RuCl_2${P(*p*-tolyl)$_3$}] precursor, whose reactions with R-DAB in toluene gave dinuclear trichloro-bridged Ru(II) complexes [Ru_2Cl_3(P(*p*-tolyl)$_3$)$_2$(R-DAB)$_2$](BF_4) which have been characterized by spectroscopic methods. In addition, one of the complexes was characterized using X-ray crystallography. Meanwhile, two mononuclear Ru(II) complexes [$RuCl_2$(P(*p*-tolyl)$_3$)$_2$(R-DAB)] were obtained from the reactions of the [$RuCl_2${P(*p*-tolyl)$_3$}] precursor with R-DAB ligands in THF. The two *trans*-mononuclear complexes were characterized by X-ray crystallography and solid-state ^{31}P NMR. A temperature-dependent ^{31}P NMR study was carried out to monitor the formation of dinuclear and mononuclear complexes.

Introduction

A number of derivatives of 1,4-diaza-1,3-butadiene, also known as diazabutadiene (R-DAB), and their complexes have been reported in the past decades [1–6]. Coordination between the R-DAB ligand and metal centre generally occurs through the two nitrogen atoms of the imine groups, giving complexes with five-membered chelate rings [1, 7]. Such five-membered chelate ring ruthenium complexes have drawn significant attention in view of the remarkable photophysical properties of ruthenium bipyridine (bpy) complexes [8–12]. However, compared with ruthenium bpy complexes, the synthesis of ruthenium R-DAB complexes is much less documented. This can in part be attributed to the formation of dinuclear ruthenium complexes instead of the mononuclear analogues. Although several dinuclear ruthenium R-DAB complexes were reported in the 1980s and 1990s, [4, 13–16], mononuclear ruthenium R-DAB complexes are more rare. In 1980, Chaudret and Poilblanc [13] reported the formation of dinuclear ruthenium R-DAB complexes with three proposed structures; but they could not identify the exact structures of these complexes. In 2014, Ghosh and co-workers reported mononuclear ruthenium R-DAB complexes obtained from the reaction between the precursor complex dichlorotris[tri(*p*-{tolyl})phosphine] ruthenium(II), [$RuCl_2${P(*p*-tolyl)$_3$}$_3$ and R-DAB ligands [17]. Surprisingly, although we used similar methodology to that reported by Ghosh et al. in our own subsequent studies, the ruthenium R-DAB complexes obtained were dinuclear analogues rather than the mononuclear molecules. This has drawn our interest to further investigate the formation of dinuclear as well as mononuclear ruthenium R-DAB complexes by using the R-DAB ligands as shown in Scheme 1. In addition, a ^{31}P NMR temperature-dependent study has been carried out in order to gain insight into the formation of dinuclear versus mononuclear complexes. The outcome of these experiments is presented herein.

Electronic supplementary material The online version of this article (https://doi.org/10.1007/s11243-018-00293-0) contains supplementary material, which is available to authorized users.

✉ Meng Guan Tay
mgtay@unimas.my

[1] Faculty of Resource Science and Technology, Universiti Malaysia Sarawak, 94300 Kota Samarahan, Sarawak, Malaysia

Published online: 17 December 2018

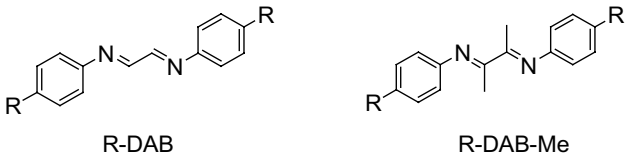

Scheme 1 Diazabutadiene compounds used in this study, R = OMe or Me

Experimental

Materials and methods

All of the complexes were synthesized using standard Schlenk techniques. $RuCl_3 \cdot nH_2O$ was purchased from Precious Metals Online and used without further purification. All other starting materials were purchased from commercial sources such as Sigma-Aldrich and Merck. The chemicals were generally used without further purification except for *p*-tolyl phosphine which was recrystallized from hot ethanol prior to use. All the solvents were dried by standard procedures and degassed. $[RuCl_2\{P(p\text{-tolyl})_3\}_3]$ was synthesized according to the method reported by Linn [18]. Toluene was purified with an Innovative Technology Inc. Pure-Solv 400 Solvent Purification System. THF-d_8 was dried by reflux over potassium for a day and then distilled. The NMR spectra were recorded using either Bruker Avance 500 MHz, Bruker Avance 300 MHz or JEOL 500 MHz NMR spectrometers. Mass spectra were obtained using an Agilent 7890A/5975C Inert GC/MSD or Varian 320 MS-GC/MS systems operating in EI mode. Mass spectrometric analysis was performed on complexes 1–4 using the MALDI technique on an Autoflex Bruker Daltonic instrument. The matrix used was 2-[(2E)-3-(4-tert-butylphenyl)-2-methylprop-2-enylidene] malononitrile (DCTB) 1:3 in THF. The high-resolution mass spectra, MS–ESI, were recorded on a Thermo Scientific Exactive™ Plus Orbitrap Mass Spectrometer. ESI measurements were taken using a HESI Source with an Aux-Gas temperature of 50 °C. ASAP/APCI measurements were taken using an APCI Source with Corona Needle and Aux-Gas temperature of 400 °C. Electronic spectra were recorded on a PerkinElmer Lambda-40-UV–Vis spectrometer with 1-cm quartz cuvettes in the range of 200–800 nm. Elemental analyses were obtained on a Firma Elementar Vario MICRO Cube analyser. IR spectra were recorded using a Thermo Scientific Fourier transform infrared spectrometer (FTIR) model—Nicolet iS10 on KBr discs in the range of 4000–400 cm^{-1}.

Crystal structure determinations

The crystal data were collected on a Bruker X8-APEX II diffractometer with a CCD area detector and multi-layer mirror/graphite-monochromated $Mo_{K\alpha}$ radiation. The structures were solved using intrinsic phasing methods [19] refined with the ShelXL program [20] and expanded using Fourier techniques. All non-hydrogen atoms were refined anisotropically. Hydrogen atoms were included in structure factor calculations. All hydrogen atoms were assigned to idealized geometric positions.

Preparation of the R-DAB compounds

The R-DAB compounds (where R = OMe or Me) were synthesized according to literature procedures with slight modifications [21] as follows.

Preparation of 1,4-di(4-methoxyphenyl)-1,4-diaza-1,3-butadiene (OMe-DAB)

Glyoxal (1.27 g, 8.76 mmol) and *p*-methoxyaniline (2.155 g, 17.5 mmol) were stirred in distilled ethanol (20 mL) at room temperature for 4 h. The yellow precipitate was collected and recrystallized by vapour diffusion of hexane into a saturated dichloromethane solution. Yield: 1.91 g, 81%. Anal. Calcd. for $C_{16}H_{16}N_2O_2$: C, 71.6; H, 6.0; N, 10.5; Found: C, 71.6; H, 6.0; N, 10.4%. ^{1}H NMR (500 MHz, DMSO-d_6, ppm): 3.79 (s, 6H, OCH_3), 7.00 (d, 4H, J = 9 Hz, H_{Ar}), 7.42 (d, 4H, J = 9 Hz, H_{Ar}), 8.46 (s, 2H, HC=N). ^{13}C NMR (125 MHz, DMSO-d_6, ppm): 159.37, 157.58, 142.55, 123.32, 114.68, 55.48. IR (KBr, cm^{-1}): 2964(w); 1607(s); 1499(s); 1285(m); 1250(m). UV–Vis (CH_2Cl_2 λ_{max}/nm): 238, 297 and 375.

Preparation of 1,4-di(4-methylphenyl)-1,4-diaza-1,3-butadiene (Me-DAB)

Glyoxal (1.27 g, 8.76 mmol) and *p*-toluidine (1.881 g, 17.5 mmol) were stirred in distilled ethanol (20 mL) at room temperature for 4 h. Work-up as above gave Me-DAB. Yield: 1.53 g, 74%. Anal. Calcd. for $C_{16}H_{16}N_2$: C, 81.3; H, 6.8; N, 11.9; Found: C, 80.6; H, 6.7; N, 11.8%. ^{1}H NMR (500 MHz, DMSO-d_6, ppm): 2.34 (s, 6H, CH_3), 7.25 (d, 8H, J = 8 Hz, H_{Ar}), 8.44 (s, 2H, HC=N). ^{13}C NMR (125 MHz, DMSO-d_6, ppm): 159.12, 147.20, 137.62, 129.94, 121.49, 20.72. IR (KBr, cm^{-1}): 2912(w); 1607(s); 1500(s); 1304(m). UV–VIS (CH_2Cl_2 λ_{max}/nm): 237, 289 and 349.

Preparation of 1,4-di(4-methoxyphenyl)-1,4-diaza-2,3-methyl-1,3-butadiene (OMe-DAB-Me)

A mixture of 2,3-butanedione (0.491 g, 5.7 mmol) and *p*-methoxyaniline (1.404 g, 11.4 mmol) was stirred in methanol (15 mL) with a few drops of formic acid at room temperature. After 4 h, the precipitate was collected and washed with cold methanol. The product was recrystallized by vapour diffusion of hexane into a dichloromethane solution. Yield: 1.05 g, 62%. Anal. Calcd. for $C_{18}H_{20}N_2O_2$: C, 73.0; H, 6.8; N, 9.5; Found: C, 73.0; H, 6.6; N, 9.3%. ^{1}H NMR (500 MHz, DMSO-d_6, ppm): 2.08 (s, 6H, H_3C-C=N), 3.76 (s, 6H, OCH_3), 6.79 (d, 4H, J = 8 Hz, H_{Ar}), 6.95 (d, 4H, J = 8 Hz, H_{Ar}). ^{13}C NMR (125 MHz, DMSO-d_6, ppm): 167.65, 155.98, 143.40, 120.66, 114.23, 55.11, 15.17. IR (KBr, cm^{-1}): 2961(w); 1632(s); 1500(s); 1240(s). UV–Vis (CH_2Cl_2 λ_{max}/nm): 292 and 350.

Preparation of 1,4-di(4-methylphenyl)-1,4-diaza-2,3-methyl-1,3-butadiene (Me-DAB-Me)

A mixture of 2,3-butanedione (0.981 g, 11.4 mmol) and *p*-toluidine (2.443 g, 22.8 mmol) was stirred in methanol (20 mL) with a few drops of formic acid at room temperature. Work-up as described above gave Me-DAB-Me. Yield: 1.68 g, 56%. Anal. Calcd for $C_{18}H_{20}N_2$: C, 81.8; H, 7.6; N, 10.6; Found: C, 81.5; H, 7.5; N, 10.7%. ^{1}H NMR (500 MHz, DMSO-d_6, ppm): 2.06 (s, 6H, H_3C-C=N), 2.30 (s, 6H, CH_3), 6.71 (d, 4H, J = 8 Hz, H_{Ar}), 7.18 (d, 4H, J = 8 Hz, H_{Ar}). ^{13}C NMR (125 MHz, DMSO-d_6, ppm): 167.60, 148.00, 132.80, 129.48, 118.88, 20.48, 15.11. IR (KBr, cm^{-1}): 2916(w); 1627 (s); 1500(m); 1361(m). UV–Vis (CH_2Cl_2 λ_{max}/nm): 336.

Preparation of dichlorotris(tri(*p*-tolyl)phosphine) ruthenium(II)

A mixture of $RuCl_3 \cdot nH_2O$ (1.70 g, 6.46 mmol) and excess tri(*p*-tolyl)phosphine (7.90 g, 11.20 mmol) in dried ethanol (70 mL) was refluxed for 3 h under argon. Schlenk filtration yielded a brown precipitate which was washed three times with hot ethanol and then twice with Et_2O. Yield: 2.8 g, 85%. ^{31}P{^{1}H} NMR (202 MHz, THF-d_8, ppm): −7.56 (s, P{*p*-tolyl}$_3$) 23.58 (s, [$RuCl_2${P(*p*-tolyl)$_3$}$_3$]). ^{1}H NMR (500 MHz, THF-d_8, ppm): 7.22 (d, 6H, J = 8 Hz, Ar–H), 6.75 (d, 6H, J = 8 Hz, Ar–H), 2.24 (s, 9H, $–CH_3$). IR (KBr, cm^{-1}): 3020, 1599, 1499, 805, 523, 461.

Preparation of complex 1

To a 100-mL Schlenk tube containing the ruthenium precursor (0.2214 g, 0.204 mmol), solid OMe-DAB (0.0536 g, 0.2 mmol) was added under argon. Dried toluene (20 mL) was then added through a syringe, and the mixture was refluxed for 2 h. The solvent was removed by concentration to 5 mL. Hexane was added to precipitate the product, which was isolated by filtration. The dark brown powder was washed with hexane and dried under vacuum. Yield: 0.20 g, 67%. ^{31}P{^{1}H} NMR (202 MHz, $CDCl_3$, ppm): 39.14 (s, 2P, [Ru_2Cl_3(P(*p*-tolyl)$_3$)$_2$(OMe-DAB)$_2$]$^+$). ^{1}H NMR (500 MHz, $CDCl_3$, ppm): 8.31 (s, 2H, –HC=N), 6.87 (d, J = 8 Hz, 8H, Ar–H), 6.75 (d, J = 8 Hz, 6H, Ar–H), 6.64 (dd, J = 8, 18 Hz, 14H, Ar–H), 3.92 (s, 8H, $–OCH_3$), 2.33 (s, 9H, $–CH_3$). MS-MALDI (*m*/*z*): 1453.23, [Ru_2Cl_3(P(*p*-tolyl)$_3$)$_2$(OMe-DAB)$_2$]$^+$. IR (KBr, cm^{-1}):1601, 1502, 1456, 1252, 831, 526, 445. UV–Vis (CH_2Cl_2 λ_{max}/nm): 248, 406 and 545.

Preparation of complex 2

A Schlenk tube was charged with Me-DAB (0.0472 g, 0.2 mmol) and the ruthenium precursor (0.2214 g, 0.204 mmol) to prepare complex 2 by a method similar to that used for complex 1. Yield: 0.18 g, 63%. ^{31}P{^{1}H} NMR (202 MHz, $CDCl_3$, ppm): 38.50 (s, 2P, [Ru_2Cl_3(P(*p*-tolyl)$_3$)$_2$(Me-DAB)$_2$]$^+$). ^{1}H NMR (500 MHz, $CDCl_3$, ppm): 8.30 (s, 2H, –HC=N), 6.90 (d, J = 8 Hz, 4H, Ar–H), 6.84 (d, J = 8 Hz, 6H, Ar–H), 6.66 (d, J = 7 Hz, 4H, Ar–H), 6.56 (dd, J = 8 Hz, J = 8 Hz, 6H, Ar–H), 2.48 (s, 6H, $–CH_3$), 2.32 (s, 9H, $–CH_3$). MS-MALDI (*m*/*z*): 1391.25, [Ru_2Cl_3(P(*p*-tolyl)$_3$)$_2$(Me-DAB)$_2$]$^+$. IR (KBr) (cm^{-1}): 1599, 1501, 1463, 810, 510, 444. UV–Vis (CH_2Cl_2 λ_{max}/nm): 235, 378 and 533.

Preparation of complex 3

A Schlenk tube was charged with OMe-DAB-Me (0.0622 g, 0.2 mmol) and the ruthenium precursor (0.2214 g, 0.204 mmol) to prepare complex 3 by a method similar to that used for complex 1. Yield: 0.16 g, 52%. ^{31}P{^{1}H} NMR (202 MHz, $CDCl_3$, ppm): 38.7(s, 2P, [Ru_2Cl_3(P(*p*-tolyl)$_3$)$_2$(OMe-DAB-Me)$_2$]$^+$). ^{1}H NMR (500 MHz, $CDCl_3$, ppm): 7.05 (s, 2H, Ar–H), 6.87 (d, J = 7 Hz, 4H, Ar–H), 6.84 (d, J = 7 Hz, 4H, Ar–H), 6.43 (broad doublet, J = 6 Hz, 10 H, Ar–H), 3.92 (s, 6H, $–OCH_3$), 2.34 (s, 5H, $–CH_3$), 2.16 (s, 2H, $–CH_3$). MS-MALDI (*m*/*z*): 1511.38, [Ru_2Cl_3(P(*p*-tolyl)$_3$)$_2$(OMe-DAB-Me)$_2$]$^+$. IR (KBr, cm^{-1}): 1604, 1503, 1246, 807, 526, 445. UV–Vis (CH_2Cl_2 λ_{max}/nm): 241, 380 and 507.

Preparation complex 4

A mixture of Me-DAB-Me (0.0528 g, 0.2 mmol) and the ruthenium precursor (0.2214 g, 0.204 mmol) was used to prepare complex 4 according to the procedure used for complex 1. A light brown precipitate was collected. Yield:

0.19 g, 64%. $^{31}P\{^{1}H\}$ NMR (202 MHz, $CDCl_3$, ppm): 38.5 (s, 2P, $[Ru_2Cl_3(P(p\text{-tolyl})_3)_2(\text{Me-DAB-Me})_2]^+$). ^{1}H NMR (500 MHz, $CDCl_3$, ppm): 7.36 (d, 2H, J = 7 Hz, Ar–H), 7.18 (d, 2H, J = 8 Hz, Ar–H), 7.04 (d, 6H, J = 6 Hz, Ar–H), 6.68 (s, 6H, Ar–H), 6.47 (m, 4H, Ar–H), 2.39 (s, 10H, $-CH_3$ of (*p*-tolyl)phosphine), 2.23 (s, 3H, $-CH_3$ of diimine R group), 1.99 (s, 2H, $-CH_3$ of diimine backbone). MS-MALDI (*m*/*z*): 1447.39, $[Ru_2Cl_3(P(p\text{-tolyl})_3)_2(\text{Me-DAB-Me})_2]^+$. IR (KBr, cm^{-1}): 1599, 1502, 1259, 796, 526, 445. UV–VIS (CH_2Cl_2 λ_{max}/nm): 235, 258 and 504.

Preparation of complex 5

In a glove box, the ruthenium precursor (0.010 g, 9.216×10^{-6} mol) was dissolved in dried THF (1 mL), and OMe-DAB (0.005 g, 1.843×10^{-5} mol) was dissolved in diethyl ether. The clear yellow solution of OMe-DAB was layered onto the brown solution of ruthenium precursor. The sealed vial was kept at −35 °C. After several days, reddish single crystals of complex 5 were isolated, mounted in oil and subjected to X-ray crystallography analysis. Further characterization could not be carried out due to the small amount of compound obtained.

Preparation of complex 6

The synthesis of complex 6 was carried out by the same method as for complex 5, but replacing OMe-DAB with Me-DAB (0.006 g, 2.765×10^{-5} mol) which was dissolved in hexane. The purple precipitate was collected, washed with hexane and dried. Recrystallization by layering hexane onto a THF solution afforded single crystals. $^{31}P\{^{1}H\}$ NMR (solid state): 16.76, 14.59, −7.32, −9.48 (d, $^{2}J(P,P) = 330$ Hz). MS–ESI (*m*/*z*): 981.28 $[Ru(\text{Me-DAB})\{P(p\text{-tolyl})_3\}_2Cl]^+$, 677.14 $[Ru(\text{Me-DAB})Cl]^+$.

Results and discussion

Synthesis of dinuclear ruthenium complexes

The ruthenium precursor, $[RuCl_2\{P(p\text{-tolyl})_3\}_3]$, was synthesized according to the literature procedure [18]. However, tri(*p*-tolyl)phosphine, $P(p\text{-tolyl})_3$, was chosen as a substitute for triphenylphosphine in order to simplify the aromatic signals in the ^{1}H NMR spectra.

The synthesis of the ruthenium complexes was similar to that described by Ghosh et al. [17], where the R-DAB ligand and the precursor complex were refluxed in dry toluene for around 2 h (Scheme 2). We initially expected to obtain mononuclear complexes, but surprisingly, the ruthenium complexes that were isolated proved to be the dinuclear analogues. Thus, the crystallographic data showed that

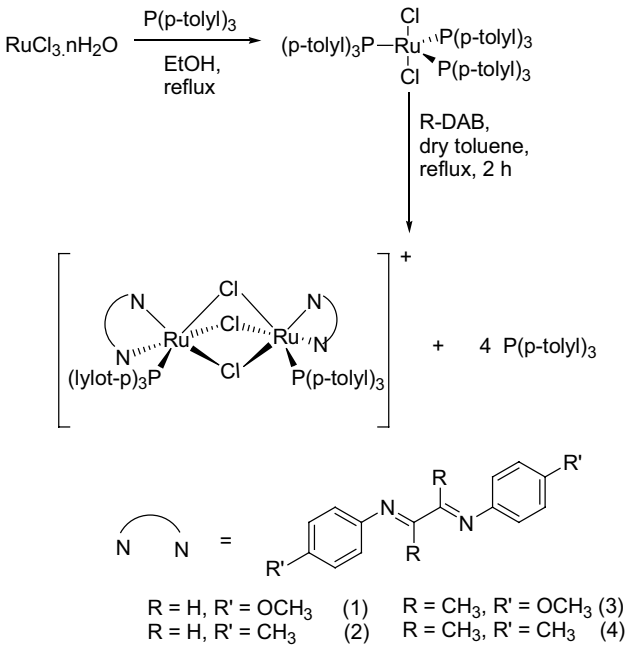

Scheme 2 Preparation of dinuclear ruthenium R-DAB complexes from the $[RuCl_2(P\{p\text{-tolyl}\}_3)]$ precursor

the ruthenium metal centres are connected by three chloro-bridging ligands, such that each metal centre is bound to one R-DAB and one $P(p\text{-tolyl})_3$ ligand.

According to the literature [13–16], the formation of trichloro-bridged dinuclear ruthenium complexes is very common due to the stability of the resulting cation. For example, this type of complex was observed by Poilblanc and co-workers, who reported the dinuclear $[Ru_2Cl_4(PPh_3)_3(DAB)]^+$ and $[Ru_2Cl_3(PPh_3)_2(DAB)_2]Cl$ obtained from the reactions of $[RuCl_2(PPh_3)_3]$ with DAB ligands [13]. The formation of dinuclear complexes has also been reported by Cotton and Torralba, who synthesized five face-sharing bioctahedral diruthenium complexes [14]. In addition, Fogg and James have explored the reactions of a dimer precursor and two-electron donor ligands to form $[RuCl(dppb)(\mu\text{-}Cl)_3Ru(dppb)(L)]$ complexes [15].

The MALDI analysis (see Supporting Information) for complex 1 showed the parent ion peak at 1453.23, in agreement with the formula of the $[Ru_2Cl_3\{P(p\text{-tolyl})_3\}_2(\text{OMe-DAB})_2]^+$ cation. Similar results were obtained for dinuclear complexes 2, 3 and 4, where the parent ion peaks at 1391.25, 1511.28 and 1447.39, respectively, agreement with the molecular masses of the cationic dimers, excluding the chloride ion. Meanwhile, dinuclear complexes 1, 2 and 3 were resynthesized using BF_4^- as the anion in order to confirm the presence of chloride in the primary valence sphere. This was done by dissolving the respective R-DAB ligands in a small amount of toluene, then adding the ruthenium

Table 1 Analytical data for dinuclear complexes 1, 2 and 3 with BF_4^- as the anion

Complex	Formula	Obs. (calc.)		
		C%	H%	N%
1	$Ru_2Cl_3C_{74}H_{74}N_4O_4P_2BF_4$	58.9 (57.7)	5.1 (4.8)	3.9 (3.6)
2	$Ru_2Cl_3C_{74}H_{74}N_4P_2BF_4$	59.9 (60.1)	5.0 (5.1)	3.9 (3.8)
3	$Ru_2Cl_3C_{78}H_{82}N_4O_4P_2BF_4$	57.6 (58.7)	5.4 (5.2)	3.4 (3.5)

precursor $[RuCl_2\{P(p\text{-tolyl})_3\}_3]$ and stirring at room temperature overnight. After removing the solvent, the red–brown residue was washed with ether. The precipitate was dissolved in methanol, and a solution of $NaBF_4$ in methanol was added dropwise. The resulting crystals were collected by filtration. The elemental analyses data as given in Table 1 confirmed that ruthenium complexes 1, 2 and 3 retain the dimeric structure.

The UV spectrum of free OMe-DAB shows three absorption bands at 238, 297 and 375 nm. The first two bands can be attributed to the primary and secondary $\pi \rightarrow \pi^*$ transitions of the benzene fragment, whilst the peak at 375 nm is assigned to $n \rightarrow \pi^*$ transitions of the C=N chromophore [22–24]. The band at 238 nm was shifted to the lower energy region at 248 nm upon complexation, and similarly, the band at 375 nm was bathochromically shifted to 406 nm in complex 1. An additional band was observed at 545 nm in the spectrum of dinuclear ruthenium(II) complex 1, which might arise from the MLCT transitions. For complexes 2, 3 and 4, possible MLCT bands were observed at 533, 507 and 504 nm, respectively. The presence of methyl groups in the backbone of the R-DAB-Me ligands (Me-C=N) in complexes 3 and 4 conferred hypsochromic shifts on the MLCT absorption bands (as compared to those of complexes 1 and 2). This result suggests that the methyl groups increase the band gap between the π *d*-orbitals of ruthenium and π antibonding orbitals of the ligand.

In the IR spectra of the free R-DAB compounds, the C=N stretching band is located in the region of 1632–1607 cm^{-1}. The presence of methyl groups in the backbone of the diazadiene moiety (Me-C=N) gave the C=N stretching at a higher frequency, specifically 1632 cm^{-1} for OMe-DAB-Me and 1627 cm^{-1} for Me-DAB-Me. After complexation, the C=N band was shifted to lower frequencies, in the range of 1604–1599 cm^{-1}. This indicated the presence of backbonding from the Ru metal centre to the π^*orbitals of the diazadiene moiety. In addition, a Ru–N band was observed in the 445–450 cm^{-1} region in the spectra of the complexes [25].

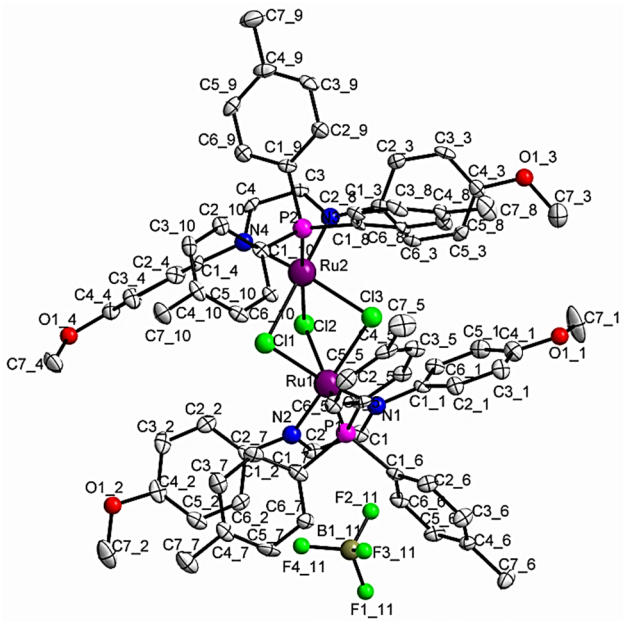

Fig. 1 Molecular structure of dinuclear ruthenium complex 2 with BF_4^- anion. Thermal ellipsoids are drawn at 50% probability. The hydrogen atoms are omitted for clarity

X-ray crystal structure of complex 2

A single crystal of the dinuclear ruthenium complex 2 with BF_4^- as the anion was collected from methanol solution after addition of $NaBF_4$ solution. The molecular structure of complex 2 is shown in Fig. 1. The Ru–N bond lengths are around 2.013–2.024 Å, slightly shorter than the value of 2.056 Å observed for $[Ru(bpy)_3]^{2+}$ [26], because the imine bond in bpy has stronger trans-influence than the chloro-bridging ligands. Meanwhile, the bond lengths within the Ru–Cl bridge are in the range of 2.405–2.496 Å, which is similar to the average reported Ru–Cl-bridging bond length of 2.428 Å [27].

Synthesis of mononuclear ruthenium complexes

Compared with the dinuclear complexes, the synthesis of mononuclear ruthenium complexes was rather more difficult. In an argon-filled glove box, the reaction of $[RuCl_2\{P(p\text{-tolyl})_3\}_3]$ with R-DAB compounds was attempted by dissolving $[RuCl_2\{P(p\text{-tolyl})_3\}_3]$ in THF and layering with a solution of the R-DAB compound in hexane. A rapid colour change from brown to purple was observed. The vial was then immediately transferred to a freezer at − 35 °C. After 1–2 days, a fine precipitate was observed; this was filtered off and washed. Solid-state $^{31}P\{^1H\}$ NMR analysis was carried out, and the spectrum in Fig. 2 shows two doublets with a coupling constant of 437 Hz for the cis isomer, which might be the reaction intermediate.

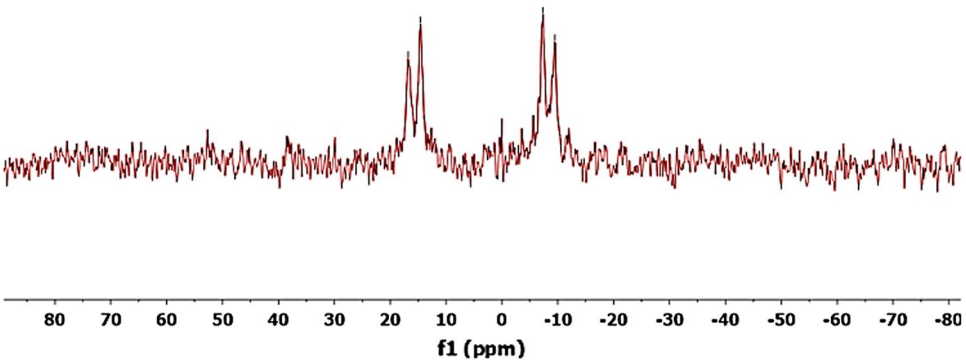

Fig. 2 Solid-state $^{31}P\{^{1}H\}$ NMR spectrum of mononuclear complex 6

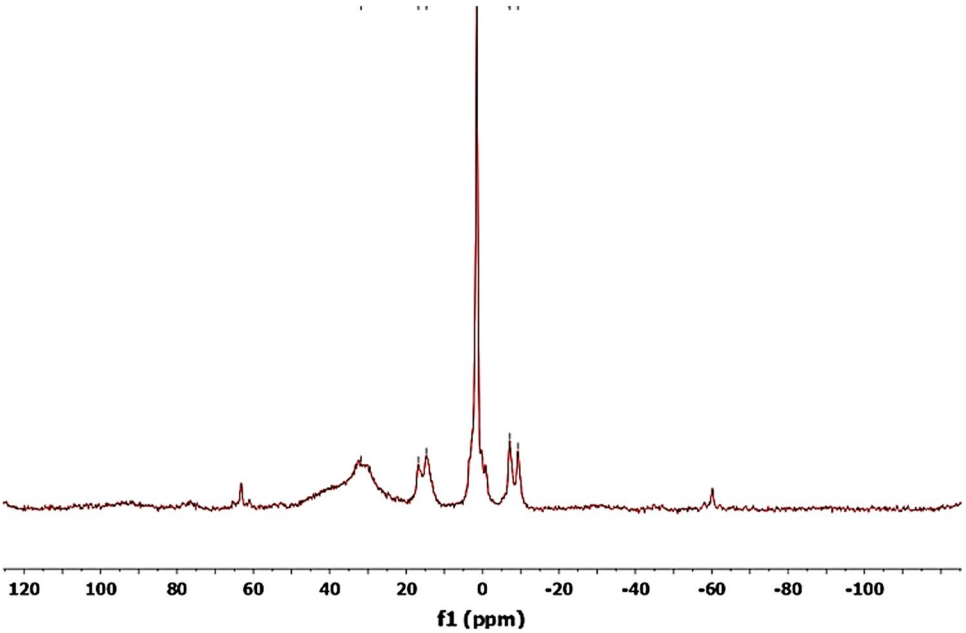

Fig. 3 Solid-state $^{31}P\{^{1}H\}$ NMR spectrum for the larger-scale synthesis of complex 6

The reaction was repeated on a large scale by reacting 150 mg of $[RuCl_2\{P(p\text{-tolyl})_3\}_3]$ with 90 mg of Me-DAB-Me. The solid-state $^{31}P\{^{1}H\}$ NMR spectrum showed a mixture (Fig. 3). Apart from the cis-intermediate which gives rise to the two doublets at $\delta = -8.16$ and $+15.75$ ppm, an intense new singlet was observed at 1.5 ppm, which is believed to be the trans-mononuclear ruthenium complex. We suspected that the mixture also contained some unreacted precursors, by comparing to the solid-state $^{31}P\{^{1}H\}$ NMR spectrum of $[RuCl_2\{P(p\text{-tolyl})_3\}_3]$. The precipitate was washed with hexane and then recrystallized by vapour diffusion of hexane into a THF solution. A single crystal was isolated thereafter, and this product exhibited the mononuclear geometry.

Meanwhile, the high-resolution mass spectrum in ESI mode (ESI–MS) showed a fragment at 981.27 g/mol corresponding to $[RuCl_2\{P(p\text{-tolyl})_3\}_2$(Me-DAB-Me)]. Notwithstanding, the trichloro-bridged dimer peak was also present at 1391.25 g/mol (see Supporting Information).

X-ray crystal structures of complexes 5 and 6

Single crystals of mononuclear complexes 5 and 6 were obtained by layering hexane onto THF solution at − 35 °C. Unlike the dinuclear complexes, the tri(*p*-tolyl)phosphine ligands in these mononuclear complexes are trans to each other, with bond angles of 177.268°–170.207°. As shown in Fig. 4, the structure of complex 5 includes two independent molecules, both of which are distorted octahedral structures. For the ruthenium complex on the left of Fig. 4a, there are two disordered diazadiene segments and two *p*-tolyl rings overlapping each other. The structure in Fig. 4 is plotted to the one with a higher site occupancy of 0.588(4). It is worth noting that the Ru–N, Ru–P, Ru–Cl, N–C and C–C bond lengths are all similar in both Ghosh's complex and our complex 5, except for Ru2–N3A (2.024 Å) and Ru2–N4A (2.099 Å), which are shorter in our complex than the one reported by Ghosh et al. (2.0519 Å). The Ru–N bond lengths for the structure in Fig. 4a are different (2.0997 and

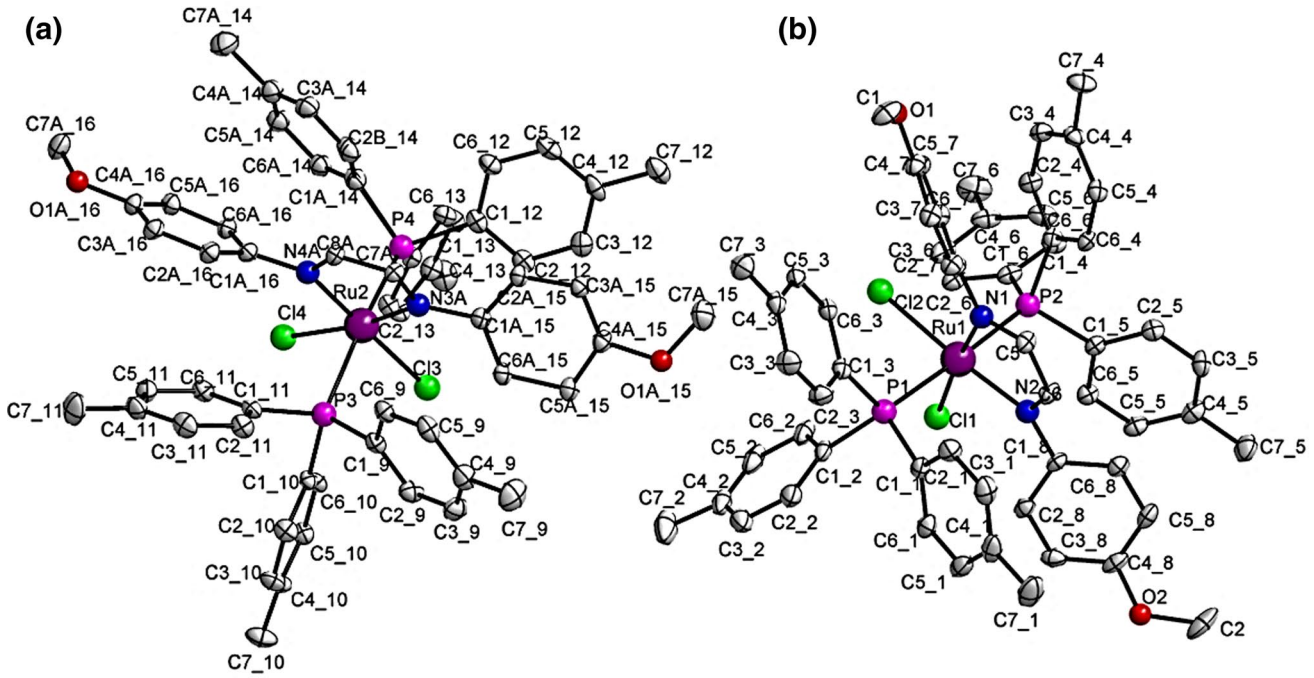

Fig. 4 Molecular structure of 5(a) and (b), with thermal ellipsoids drawn at 50% probability. The hydrogen atoms connected to carbon and the THF solvate molecules are omitted for clarity

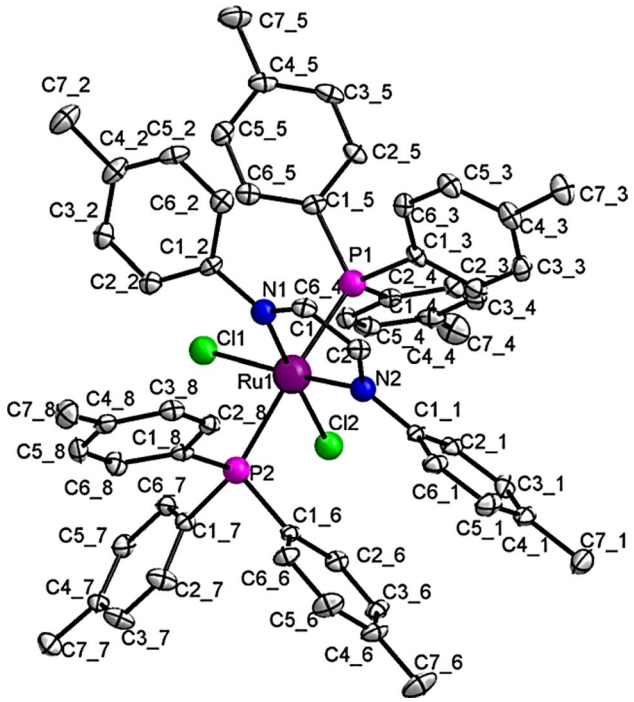

Fig. 5 Molecular structure of complex 6, with thermal ellipsoids drawn at 50% probability. The hydrogen atoms connected to carbon and two molecules of THF solvate are omitted for clarity

2.0249 Å), and this might be due to packing effects in the crystal [28]. However, the N–C and C–C bond lengths are indistinguishable in this structure.

The mononuclear complex 6 (Fig. 5) bearing a *p*-CH_3 diazadiene ligand was crystallized in an orthorhombic $Pna2_1$ space group. The bond lengths and angles in complex 6 are similar to those in complex 5. Comparing the bond lengths of the free diimines and the coordinated ligands, the –C=N–bond length increased from 1.28 to 1.31 Å upon coordination to the Ru metal centre. Conversely, the =CH–CH= bond length became shorter compared with the free diimines, from 1.45 to 1.40 Å. The free diimine showed a typical carbon–nitrogen double-bond length (1.28 Å) and carbon–carbon single bond (1.45 Å) in a Csp^2–Csp^2 conjugated system. The deformed diazadiene, showing longer –C=N– and shorter =CH–CH= bond lengths after coordination, is an indicator of strong back donation [17]. Upon coordination to the ruthenium centre, the angles C2–C1–N1 and C1–N1–C1_2 showed a slight 3° decrease from the free diazadiene (~ 119°) as the two sides of the –C=N– are brought together in order to coordinate to the metal centre.

Temperature-dependent $^{31}P\{^1H\}$ NMR study

A temperature-dependent $^{31}P\{^1H\}$ NMR experiment was carried out to determine the effect of this parameter on

Scheme 3 Equilibrium of dinuclear and mononuclear ruthenium(II) complexes

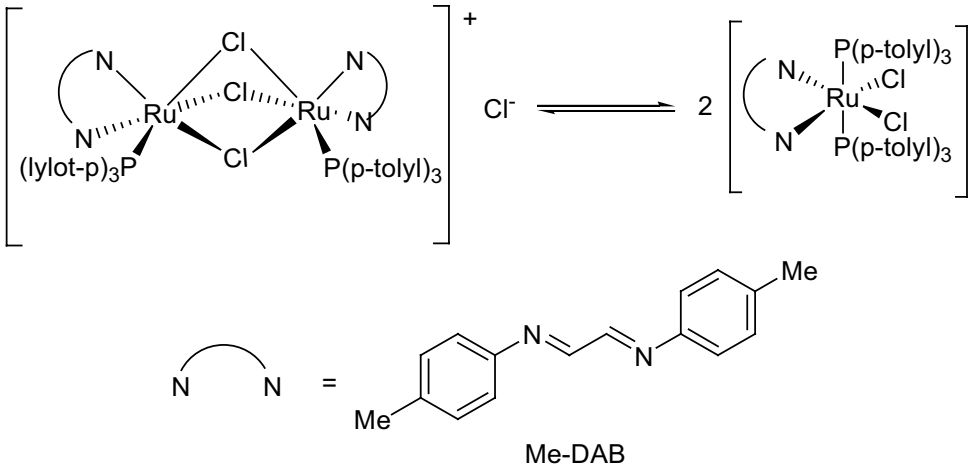

Table 2 Relative intensities of dinuclear and mononuclear complex signals with free P(*p*-tolyl)$_3$ at different temperatures

Temp (°C)	ppm		
	+31	+1	−7
+25	–	47.76	52.24
+20	Trace	52.51	47.48
+15	5.49	47.77	46.73
+10	11.75	40.69	47.56
+5	20.31	27.09	52.58
0	33.06	6.03	60.90
−20	32.02	1.21	66.76
−38.2	29.31	1.08	69.60

Signal identifications: +31 ppm dinuclear complex; +1 ppm mononuclear complex; −7 ppm free *p*(tolyl)$_3$

the formation of dinuclear and mononuclear complexes (Scheme 3). A mixture of [RuCl$_2${P(*p*-tolyl)$_3$}$_3$] and Me-DAB was placed in an NMR tube in the glove box. It was then transferred to a Schlenk line and dried THF-d$_8$ was added. The NMR tube was immediately placed in an isopropanol cold bath (−40 °C), and the reaction was monitored at different temperatures: −38.2, −20, 0, +5, +10, +15, +20 and +25 °C using ^{31}P{^{1}H} NMR spectroscopy. The analyses were performed in triplicate at each temperature before the temperature was increased. In the resulting spectra, three peaks were observed at +31 ppm (dinuclear), +1 ppm (mononuclear) and −7 ppm [free P(*p*-tolyl)$_3$]. The relative integrations of the peaks are given in Table 2. It can be seen that at a low temperature, the peak at 31 ppm, which is attributed to the dinuclear complex, has a higher intensity compared with the monomer at around 1 ppm. When the temperature was increased, the proportion of the monomer also increased, while the dimer peak gradually disappeared.

The results from the temperature-dependent ^{31}P{^{1}H} NMR study contradicted the observations made in the synthesis of the dinuclear and mononuclear ruthenium complexes, in which the dinuclear complexes were obtained at higher temperature and vice versa. However, for the dinuclear complexes, the reaction solvent was toluene, whereas THF was used for the mononuclear complexes. It is probable that the different polarities of these two solvents are responsible for the formation of dinuclear or mononuclear complexes. In a paper published by Scholz et al. [29] on R-DAB complexes, the authors stated that dinuclear complexes dissociated in THF. It was also observed that the dinuclear complexes have poor solubility in non-polar solvents such as toluene because of their monocationic nature.

Conclusions

The syntheses of dinuclear and mononuclear ruthenium complexes using R-DAB ligands with [RuCl$_2${P(*p*-tolyl)$_3$}] precursor have been demonstrated. The structures of both types of complexes have been confirmed by X-ray crystallography, NMR and MALDI. Temperature-dependent ^{31}P{^{1}H} NMR experiments showed that the dinuclear complex was more favourable at low temperature, whereas the mononuclear complex was more preferable at a higher temperature.

Supplementary data

CCDC 1871392, 1871390, 1871393 and 1871391 contain the supplementary crystallographic data of ruthenium(II) precursor, [RuCl$_2${P(*p*-tolyl)$_3$}$_3$], dinuclear ruthenium(II) complex 2 and mononuclear ruthenium(II) complexes 5 and 6, respectively. These data can be obtained free of charge from the Cambridge Crystallographic Data Centre via www.ccdc.cam.ac.uk/data_request/cif.

Acknowledgements The authors are thankful to Professor Todd B. Marder for providing us the facilities in his research laboratory. We would like to thank Dr. Martin Hähnel and Dr. Daniel Sieh for their opinion on the synthetic methods as well as sharing their knowledge on complexation. In addition to that, we are grateful to Dr. Rüdiger Bertermann for his help with the solid-state NMR analysis and Dr. Alexandra Friedrich for her help with the X-ray crystallography analysis. We would also like to thank Malaysian Ministry of Education for the financial support to the research through Exploratory Research Grant Scheme [ERGS/STG01(01)/1021/2013(01)].

References

1. Keijsper J, Poel HVD, Polm LH, Koten GV, Vrieze K (1983) Polyhedron 2:1111–1116
2. Koten GV, Jastrzebski JTBH, Vrieze K (1983) J Organomet Chem 250:49–61
3. Bildstein B, Malaun M, Kopacka H, Fontani M, Zanello P (2000) Inorg Chim Acta 300–302:16–22
4. Chaudret B, Köster H, Poilblanc H (1981) JCS Chem Commun (6):266–268
5. Rosenberger V, Dieck HT (1990) Chem Ber 123:83–85
6. Grupp A, Bubrin M, Ehret F, Zeng Q, Hartl F, Kvapilová H, Záliš S, Kaim W (2014) Eur J Inorg Chem 2014:110–119
7. Ceder RM, Muller G, Ordinas M, Font-Bardia M, Solans X (2003) Dalton Trans (15):3052–3059
8. Cannizzo A, Mourik FV, Gawelda W, Zgrablic G, Bressler C, Chergui M (2006) Angew Chem Int Ed 45:3174–3176
9. Juris A, Balzani V, Barigelletti F, Campagna S, Belser P, Zelewsky AV (1988) Coord Chem Rev 84:85–277
10. Lytle FE, Hercules DM (1969) J Am Chem Soc 91:253–257
11. Klassen DM, Crosby GA (1968) J Chem Phys 48:1853–1857
12. Bensasson R, Salet C, Balzani V (1976) J Am Chem Soc 98:3722–3724
13. Chaudret B, Poilblanc R (1980) Dalton Trans (3):539–544
14. Cotton FA, Torralba RC (1991) Inorg Chem 30:2196–2207
15. James BR, Fogg DE (1997) Inorg Chem 36:1961–1966
16. Cruz SS, Amenta DS, Gilge JW, Yap GPA (2016) Polyhedron 114:179–183
17. Patra SC, Roy AS, Manivannan V, Weyhermüller T, Ghosh P (2014) Dalton Trans 43:13731–13741
18. Linn DE Jr (1999) J Chem Educ 76:70–72
19. Sheldrick GM (2015) Acta Crystallogr C Struct Chem 71:3–8
20. Sheldrick GM (2008) Acta Crystallogr A Found Crystallogr 64:112–122
21. Zhong HA, Labinger JA, Bercaw JE (2002) J Am Chem Soc 124:1378–1399
22. Sathiyaraj S, Ayyannan G, Jayabalakrishnan C (2014) J Serb Chem Soc 79:151–165
23. Kliegman JM, Barnes RK (1970) J Org Chem 35:3140–3143
24. Bhowon MG, Li HKW, Narain R (1999) Polyhedron 18:341–345
25. Nagajothi A, Kiruthika A, Chitra S, Parameswari K (2013) Res J Chem Sci 3:35–43
26. Biner M, Bürgi HB, Ludi A, Röhr C (1992) J Am Chem Soc 114:5197–5203
27. Orpen AG, Brammer L, Allen FH, Kennard O, Watson DG, Taylor R (1989) J Chem Soc Dalton Trans 12:1–83
28. Lucaciu R, Ionescu C, Wildervanck A, Caira MR (2008) Anal Sci 24:87–88
29. Scholz J, Hadi GA, Thiele K-H, Görls H, Weimann R, Schumann H, Sieler J (2001) J Org Chem 626:243–259